Experimental study of small scale and high expansion ratio ORC for recovering high temperature waste heat

Uusitalo Antti, Turunen-Saaresti Teemu, Honkatukia Juha, Dhanasegaran Radheesh

DOI: 10.1016/j.energy.2020.118321

EXPERIMENTAL STUDY OF SMALL SCALE AND HIGH EXPANSION RATIO ORC FOR RECOVERING HIGH TEMPERATURE WASTE HEAT

Antti Uusitalo, Teemu Turunen-Saaresti, Juha Honkatukia, Radheesh Dhanasegaran

*LUT University, School of Energy Systems, Yliopistonkatu 34, P.O. Box 20, 53851 Lappeenranta, Finland

Abstract

In recent times, the use and development of small-scale (≈ 10 kW) ORC systems has received an increasing interest. However, the operational characteristics of small-scale high-expansion ratio ORC turbines are not yet well understood. In this study, a small-scale high-temperature ORC was investigated experimentally. The studied system has a high-speed turbogenerator including a supersonic radial turbine, a permanent magnet generator and a Barske-type feed pump assembled on a single shaft. Siloxane MDM is used as the working fluid. The turbogenerator performance was studied under different operating conditions and the experimental results were compared against the results obtained from the numerical ORC cycle model for validating the numerical results. The turbine was analyzed to have the mechanical power output close to the system design value and a maximum electric power output of 6 kW was measured. The turbogenerator was capable to be operated at the targeted rotational speed range of 12 000 rpm to 31 000 rpm. Thus, the technical potential of using high rotational speed and supersonic turbomachinery in small-scale and high expansion ratio ORC applications was confirmed. The results highlights the importance of reducing turbogenerator losses and internal power consumption to reach higher power outputs in the future.

Keywords: Waste Heat Recovery, Organic Rankine Cycle, Organic Fluid, Siloxane, Radial turbine

Nomenclature

Latin alphabet

A heat transfer area, m^2

h specific enthalpy, kJ/kg

$\dot{m}$ mass flow rate, kg/s

m mass, kg

n rotational speed, rpm

P power, kW

p pressure, bar

T temperature, ^{o}C

U heat transfer coefficient, W/m^2K

Greek alphabet

Email address: *Corresponding author: antti.uusitalo@lut.fi (Antti Uusitalo, Teemu Turunen-Saaresti, Juha Honkatukia, Radheesh Dhanasegaran)

η efficiency, -

Π turbine pressure ratio, -

ϕ heat rate, kW

Subscripts

e electrical

ev evaporation/evaporator

in inlet

out outlet

l losses and internal power consumption

s isentropic

t turbine

wf working fluid

Abbreviations

MDM Octamethyltrisiloxane

ORC Organic Rankine cycle

OC Operating condition

LUT Lappeenranta-Lahti University of Technology

TG Turbogenerator

1. Introduction

An organic Rankine cycle (ORC) is a Rankine cycle that uses an organic fluid as the working fluid. ORCs have typically been implemented in biomass power plants and geothermal power plants as well as for recovering industrial waste heat [1, 2]. In recent times, the use of ORCs in small-scale applications, having a power output in a range from 1 kW to 50 kW, has attracted an increasing interest. The potential applications for small-scale ORCs are heat recovery from small reciprocating engines [3], micro gas turbines [4], and the use of ORCs as domestic power units [5, 6].

The selection of the working fluid has an important role in the ORC machinery design and it highly affects the system thermodynamic properties, performance, as well as the component sizes [7, 8]. One interesting fluid group for high temperature waste heat recovery are siloxanes as it has been observed that the use of fluids with high molecular weight and high critical temperature allows to reach high cycle efficiencies in low-power output and high-temperature ORC systems [9, 10]. On the other hand, this type of fluids

are characterized by high cycle expansion ratios, significantly low condensing pressures, and small enthalpy drops over the expansion [11]. The other benefits related to the use of siloxanes include a good thermal stability, feasible sized turbine wheels at low power scale as well as good lubrication properties when liquid bearings in the turbogenerator are used [9].

One of the most notable technical challenges in small-scale ORCs is to reach high efficiency for the expander. In many small-scale ORC systems having power output range from few kW to several tens of kW, volumetric expanders, such as scroll, piston or screw expanders have been preferred instead of kinetic turbines[2, 12]. Along with the power range, the selection of the expander type is highly affected by the targeted operating conditions of the cycle [1, 2]. In general, volumetric expanders are suitable for relatively low expansion ratios [13, 14], whereas turbines can reach high expansion ratios even in single-stage turbine configurations [15]. Weiß [12] evaluated and compared different types of volumetric and turbine expanders regarding their applicability in small ORCs. It was concluded, that one of the most significant benefits of using small kinetic turbines is their ability to operate with high expansion ratio and small volume flow conditions. Thus, especially in small-scale and high temperature ORC systems, the use of turbines can be considered as an attractive technical option. Recently, Meroni et al. [16] have proposed a comprehensive methodology for the preliminary design and performance prediction of radial-inflow turbines especially for high-pressure ratio ORC applications. In this type of ORC turbines, the flow is typically highly supersonic due to the low speed of sound of the considered fluids [16, 17].

The use of small-scale kinetic ORC turbines has been recently studied but there are only few papers presenting experimental results for small-scale (well below 100 kW) ORC turbines. Weiß et al. [10] investigated experimentally the behavior of a supersonic axial impulse turbine and a radial cantilever turbine having maximum power output of about 12 kW, design pressure ratio of 19, design inlet temperature of 176 ^{o}C and using siloxane MM as the working fluid. Based on their study, a high turbine efficiency of over 75 % was reached despite the low power scale and it was concluded that turbines can be an efficient expander technology also in small-scale ORCs. Kang [18] investigated a radial turbine in a low temperature ORC having an electric power output of 30 kW, pressure ratio of 4.1 and turbine inlet temperature of 80 ^{o}C. R245fa was used as the working fluid in the experiments. According to the study by Kang [18], a relatively high turbine efficiency of 78.7 % was achieved. Klonowicz et al. [19] measured the performance of a low temperature 10 kW ORC turbogenerator including a partial admission axial turbine using R227ea as the working fluid. The measured efficiency of the power generation was 55 % that was close to the predicted efficiency value by using turbine loss correlations. Seume et al. [20] measured the performance of a small-scale ORC turbine using ethanol as the working fluid. The turbine was a partial admission axial turbine with the design inlet temperature of about 250 ^{o}C and the pressure ratio of 50. The measured total-to-static efficiency between 43.1 % and 57.0 % was measured. In addition to the previous experimental studies on small-scale ORC turbines, there are experimental facilities currently in the commissioning phase that will

be capable for investigating the operation of small-scale high-temperature ORC turbines [21].

Despite the previous experimental studies regarding the operation of small-scale ORC turbines, the experimentally validated operational characteristics of high-temperature (above 200 ^{o}C) and high expansion ratio radial turbines for ORC applications seems to be missing in the present literature. In this study, experimental results of a micro-ORC system producing electric power from high-temperature waste heat and using siloxane MDM as the working fluid are presented and analyzed. The system has a high speed turbogenerator containing a high expansion ratio radial turbine, a feed pump and a high-speed generator. The performance of the process heat exchangers were examined in [22] and thus, the main focus of this paper is on analysing the performance of the high-speed turbogenerator for producing electric power from the vapor expansion. The novelty of the paper is to experimentally investigate the operation of small-scale and high expansion ratio supersonic radial turbine and the turbogenerator performance under different operating conditions and with variable turbogenerator rotational speeds. In addition, the internal power consumption and losses in the system turbogenrator are investigated. The paper highlights and discusses the main advantages and specific operational characteristics of the studied ORC system as well as discusses the key aspects for further reducing losses in ORC systems adopting small-scale and high rotational speed turbomachinery. The studied ORC power range of 5 kW to 10 kW is particularly interesting for high temperature waste heat recovery from exhaust gases of 100-200 kW scale reciprocating engines or micro gas turbine systems of about or below 100 kW scale.

2. Experimental system and methods

The experiments were carried out by using an ORC test bench at Lappeenranta-Lahti University of Technology (LUT). The main componets of the experimental ORC cycle are a turbogenerator, evaporator, recuperator, condenser, condensate tank, and pre-feed pump. The system has a high-speed turbogenerator (TG) having a supersonic high expansion ratio radial turbine, a permanent magnet generator and a Barske-type feed pump, which is the main feed pump of the ORC system, assembled on a single shaft. The turbogenerator bearings are lubricated by using the liquid working fluid and the generator is cooled by using low pressure working fluid vapor. The rotational speed of the turbogenerator is controlled via a frequency converter. The experimental facility is presented in Figure 1a showing the placement of the main components. A simplified process diagram of the experimental system is shown in Figure 1b. The turbine and the main feed pump impeller are presented in Figure 2a and 2b. The turbogenerator of the ORC system is presented in Figure 2c. As the main feed pump and the turbine are assembled on a single shaft the increase in TG rotational speed increases the evaporation pressure in the system as well as affects the turbine operation. The turbine has a highly supersonic stator (Ma=2.2 at the design conditions) and MDM has a relatively low critical pressure ratio which leads to chocked conditions at the turbine stator throat

at the studied operating conditions. Thus, the mass flow through the system is mainly dependent on the mass flow rate through the turbine stator throat, and is rather insensitive to the changes on the conditions downstream the turbine. The pre-feed pump is used for increasing the pressure at the main feed pump inlet in order to avoid fluid cavitation in the main feed pump and also for providing sufficient flow through the TG bearings when starting the system. The heat source of the system is about 400 ^{o}C exhaust gas from a 150 W to 200 kW scale diesel engine and the heat energy is extracted from the exhaust gas to the working fluid in the system evaporator with a direct evaporation without any intermediate heat transfer loop. Water at about 10 ^{o}C is used as the condenser coolant.

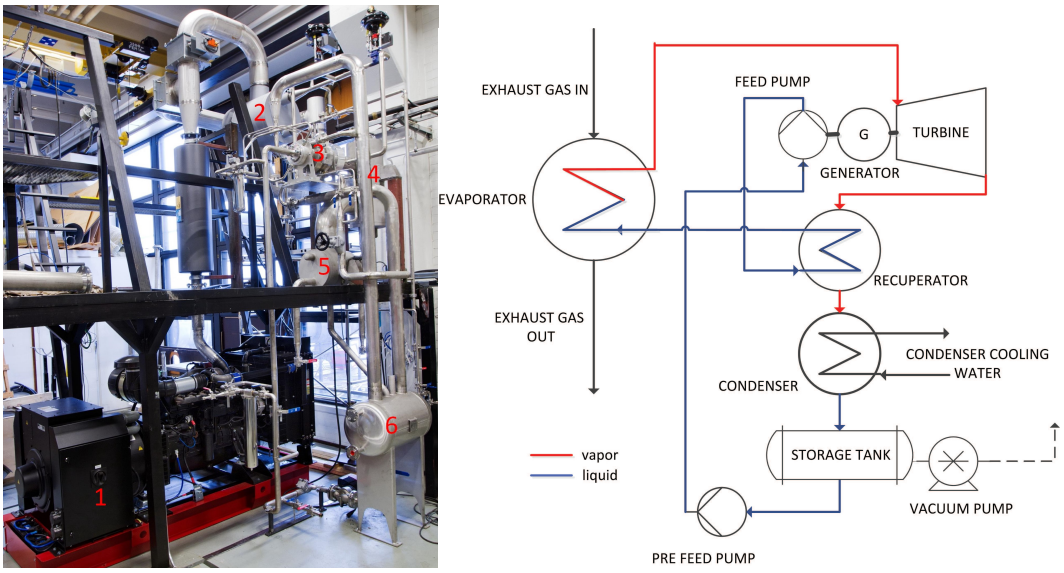

(a) (b)

Figure 1: (a) Experimental facility, (1) diesel generator, (2) evaporator, (3) turbogenerator, (4) recuperator, (5) condenser and (6) condensate tank. (b) A simplified process diagram of the experimental system.

The system design operating conditions and saturation curves of siloxane MDM are shown in Figure 3 on temperature-entropy plane. The design operational values of the experimental facility are summarized in Table 1, turbine geometry and design parameters are shown in Table 2, and the heat exchanger design parameters are shown in Table 3. More information on the selection of the working fluid for the experimental setup can be found in reference [9] and the selection of system design values and design methods are described in more detail in references [22] and [23].

The experiments were carried out with varying operating conditions. During the experiments, the ORC operating conditions were controlled by varying the TG rotational speed via a frequency converter and by varying the diesel generator load. The evaporation pressure and working fluid mass flow rate in the system were controlled by adjusting the TG rotational speed. The diesel engine generator power output

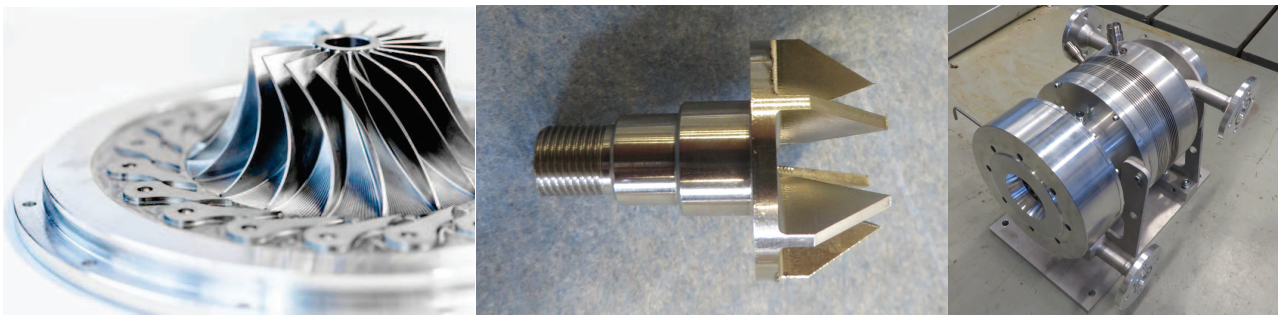

(a) (b) (c)

Figure 2: (a) Turbine stator and rotor wheel, (b) main feed pump impeller, and (c) turbogenerator including the radial turbine, main feed pump and generator.

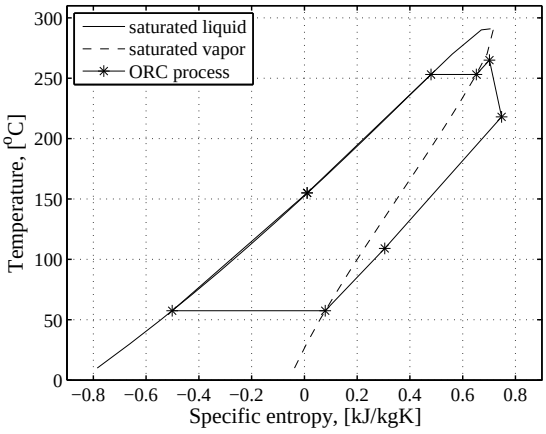

Figure 3: Experimental system design conditions and saturation curves of MDM on temperature-entropy plane.

was varied between 120 kW to 210 kW in the experiments to reach sufficient evaporator heat rate for the different operating conditions as well as for controlling the degree of superheating in the evaporator. In addition, the valve opening distributing the liquid working fluid to the TG bearings and to the evaporator was controlled during the tests. The cooling water flow through the condenser was kept as constant. The working fluid pressure and temperature were measured at different parts of the process, mainly at the inlet and outlet of each process component by using commercial pressure transducers and temperature sensors. The flow rate was measured by using a positive displacement meter as the primary flow rate measurement and an orifice as a secondary measurement. The electric power output of the system was defined from the frequency converter. The measurement equipment used in the experimental facility for measuring pressure, temperature and flow rate are presented in Table 4.

Based on the measured temperatures and pressures, the fluid enthalpy at each respective process node was calculated by using the commercial thermodynamic library Refprop[24]. The mechanical power produced

Table 1: Experimental system design values [22, 23]. *A pressure drop of 0.04 bar was estimated to occur between the turbine outlet and the condenser at the design operating condition.

Working fluid	MDM
Working fluid mass flow rate [kg/s]	0.2
Turbine mechanical power [kW]	≈ 12
Electric power output [kW]	≈ 8
Evaporator heat rate [kW]	67
Recuperator heat rate [kW]	40
Turbine inlet pressure [bar]	7.9
Turbine inlet temperature [^{o}C]	265
Turbine outlet pressure [bar]*	0.07
Turbine outlet temperature [^{o}C]	≈ 220
Condensing pressure [bar]*	0.03
Condensing temperature [^{o}C]	57
TG rotational speed [rpm]	31500

Table 2: Turbine geometry and design parameters [23].

Estimated isentropic efficency [%]	76
Turbine rotor inlet diameter [mm]	144.0
Blade height at the rotor inlet [mm]	2.0
Blade height at the rotor outlet [mm]	28.5
Number of rotor blades [-]	18
Number of stator vanes [-]	19
Mach number at the stator outlet [-]	2.2

by the turbine was evaluated by using the measured working fluid mass flow rate as well as the measured temperature and pressure at the turbine inlet and outlet. By using the measured turbine inlet and outlet pressures and temperatures, the enthalpy change over the expansion was estimated. The mechanical power of the turbine is calculated as

$$P_{\mathrm{t}} = \dot{m}_{\mathrm{wf}}(h_{\mathrm{t,in}} - h_{\mathrm{t,out}}). \tag{1}$$

Table 3: Heat exchanger design values [22].

Heat exchanger	Type	A, [m^2]	U, [W/m^{2}K]	m, [kg]	ΔT_{LMTD}, [K]
Evaporator	Plate-Shell	30.4	31	515	72
Recuperator	Plate-Shell	16.0	43	218	59
Condenser	Plate-Shell	7.0	201	168	40

Table 4: Measurement equipment.

	Manufacturer	Type	Accuracy
Pressure	Gems	2200, [0-1,0-4,0-10,0-16 bar(abs)]	± 0.25%
Pressure	Wika	A10, 0-6 bar(abs)	± 0.25%
Temperature	Aplisens	GT-GN1	± 0.35 K (at 100 ^{o}C temperature)
Flow rate	Kytola Instruments	oval gear SRP-40-H	± 0.5%

The turbine isentropic efficiency is calculated as

$$\eta_{\mathrm{s}} = \frac{(h_{\mathrm{t,in}} - h_{\mathrm{t,out}})}{(h_{\mathrm{t,in}} - h_{\mathrm{t,out,s}})}. \tag{2}$$

The ORC cycle thermal efficiency was defined as

$$\eta_{\mathrm{cycle}} = \frac{P_{\mathrm{t}} - P_{\mathrm{p}}}{\phi_{ev}} \tag{3}$$

,

and the ORC electric efficency was defined as

$$\eta_{\mathrm{e}} = \frac{P_{\mathrm{e}}}{\phi_{ev}}. \tag{4}$$

The power consumption of the pre-feed pump was not taken into account in defining the efficiencies.

In a more detailed analysis of TG internal losses and internal power consumption, the power consumption of the main feed pump and of the generator cooling fan as well as the losses in the turbogenerator including the electrical and mechanical losses were evaluated by using the measured electric power output and the calculated turbine mechanical power as follows

$$P_{\mathrm{l}} = P_{\mathrm{t}} - P_{\mathrm{e}}. \tag{5}$$

The turbogenerator losses and internal power consumption obtained from eq. 3 were compared to the ones that were estimated in the system design phase. The turbogenerator losses and internal power consumption were estimated in the system design phase for the different turbogenerator parts, including the generator, generator cooling fan, feed pump, and bearings. In addition, the magnitude of windage losses and other frictional losses were estimated based on the final turbogenerator geometry, rotational speed and fluid density at the different parts inside the turbogenerator. Before the experiments with the full setup, the performance of the electric generator was tested separately, whereas the other turbogenerator components have been tested only with the full turbogenerator assembly.

3. Results and Discussions

The analysis of the experimental results is presented in the following. The turbine inlet pressure was ranging from 3 bar to 8 bar, and the turbine inlet temperatures were ranging from about 240 ^{o}C to 280 ^{o}C in the experiments. The mass flow rate of the working fluid was ranging from about 0.1 kg/s to over 0.2 kg/s in the experiments. Both fluid states close to the saturated state at the turbine inlet and superheated state at the turbine inlet were investigated. Examples of the measured cycle operating conditions are presented in Figures 4a and 4b. As MDM has an overhanging saturated vapor curve, the turbine expansion occurred completely in the superheated vapor region in all the studied operating conditions.

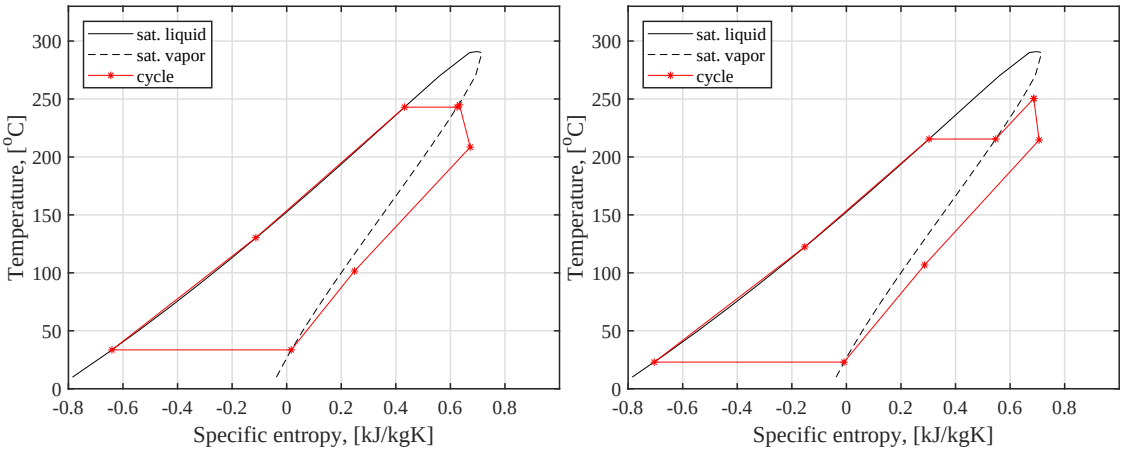

Figure 4: ORC process on T,s plane. Figure (a) is for saturated turbine inlet conditions and Figure (b) for superheated turbine inlet conditions.

The component and cycle performances defined from the measurements for seven cycle operating conditons (OC) are presented in Table 5. The selected OCs have rather stabilized conditions with no significant fluctuations in the measured data. TG rotational speed is ranging from 23500 to 31300 rpm, working fluid

mass flow rate is ranging from 0.17 kg/s to 0.22 kg/s and the evaporator outlet pressure is ranging from 6.0 bar to 7.4 bar in the presented data in Table 5. In OC3 and OC7 the condenser pressure level and the turbine outlet pressure are higher when compared to the other OCs. In general, the measured cycle conditons, heat exchanger performances and turbine mechanical power outputs close to the system design values were reached in the experiments. In the data in Table 5 the highest turbine power output of 11.0 kW was defined (OC5) and the highest electric power output of 5.9 kW was reached in OC1. It should be noted that slightly higher turbine power outputs of over 12 kW and electric power output of 6 kW were measured during the experiments but these operating conditions are not presented in Table 5 due to some fluctuations in the measured operating parameters. The cycle thermal efficiencies defined from the measurements were in the range of 11 % to 14 % for OC1-OC7 whereas the electric efficencies in the respective operating conditions were significantly lower being in the range of 4 % to slightly below 8 %. This is due to the electric power output of the system being significantly lower than the turbine mechanical power output. The highest electric power outputs were reached with TG rotational speeds well below the design rotational speed whereas the electric power output is decreased at higher TG rotational speeds. The TG performace, internal losses, internal power consumption and the turbine performance at different operating conditions are presented and discussed in more detail later in this section. The performance of the system heat exchangers have been investigated and analyzed in more detail in reference [22] and thus, the following analysis will be concentrated on the TG.

One of the most important process components in the experimental system is the main feed pump of Barske type. It is essential for the system that the feed pump is capable to increase the pressure level of the fluid to reach high evaporation temperature when the TG is running at high speed. As the turbine is supersonic and it has chocked flow conditions the high pressure is needed to have high mass flow rate through the turbine stator throat. The measured main feed pump outlet pressure as a function of TG rotational speed is presented in Figure 5 that includes the data points obtained from the measurements of several test runs. Thus, Figure 5 shows the trend where the main feed pump outlet pressure increases as the turbogenerator rotational speed increases. The mass flow rates were not always constant at the same rotational speeds which appears in variations of feed pump outlet pressure at the same rotational speeds in Figure 5. The variations can be explained by the differences in the valve opening which distributes a part of the flow to the TG bearings and the rest of the flow to the evaporator. In the measurements, it was observed that the pump can reach the design evaporator inlet pressure of over 8 bar with the system design mass flow rate of 0.2 kg/s.

The measured electric power output as a function of turbine inlet pressure and mass flow rate is presented in Figure 6 for different operating conditions. The maximum electric power output reached in the test runs was about 6 kW that is about 2 kW lower than the design power rating defined in the ORC system design phase. In general, a clear dependency in the measured electric power on the turbine inlet pressure and fluid

Table 5: Selected operational conditions and results.

	OC1	OC2	OC3	OC4	OC5	OC6	OC7
n_{TG} [rpm]	23500	23513	26356	27060	28843	30629	31325
P_{t}, [kW]	10.1	8.2	8.4	10.8	11.0	10.6	9.7
P_{e}, [kW]	5.9	4.9	3.6	4.7	4.5	4.3	3.2
ϕ_{ev}, [kW]	76.3	66.0	56.9	71.0	70.5	74.8	75.5
ϕ_{rec}, [kW]	39.9	34.9	33.5	41.9	41.4	43.4	41.3
ϕ_{cond}, [kW]	66.0	56.7	49.8	60.2	60.0	63.8	65.4
η_{cycle}	12.0	11.2	13.5	14.1	14.4	13.0	11.7
η_{elec}	7.7	7.5	6.3	6.6	6.4	5.7	4.2
$\dot{m}_{\mathrm{m,wf}}$, [kg/s]	0.22	0.19	0.17	0.20	0.20	0.21	0.22
$p_{\mathrm{ev,out}}$, [bar]	7.9	6.7	6.0	6.6	6.7	7.0	7.4
$T_{\mathrm{ev,out}}$, [^{o}C]	248.8	245.0	242.2	258.1	254.6	252.7	249.6
$T_{\mathrm{t,out}}$, [^{o}C]	212.8	208.5	211.7	220.9	217.6	215.4	214.3
Π [-]	58.4	71.9	36.3	67.5	69.8	70.6	38.7
T_{cond}, [^{o}C]	42.5	33.5	39.0	32.2	34.1	34.1	47.5
p_{cond}, [bar]	0.07	0.05	0.10	0.05	0.05	0.05	0.13

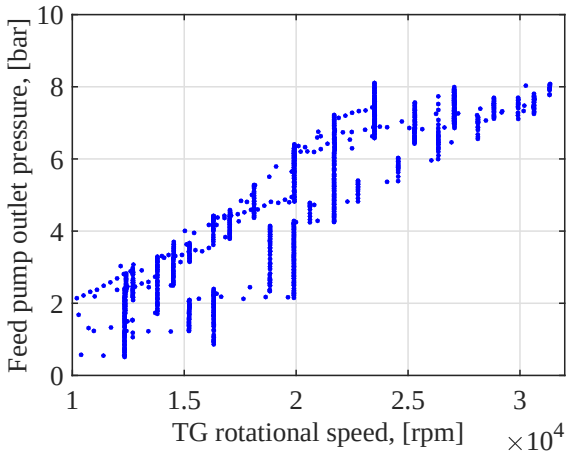

(a)

Figure 5: Measured main feed pump outlet pressure as a function TG rotational speed.

mass flow rate was observed but the electric power output is also sensitive on the TG rotational speed. Also, a dependency in the estimated turbine mechanical power on the above-mentioned parameters was observed

in the analysis of the test results, although the relation was not as clear as with the measured electric power output as shown in Figure 6. This can be explained by the fluctuations in the turbine inlet and outlet temperature measurements that affect the calculated turbine mechanical power.

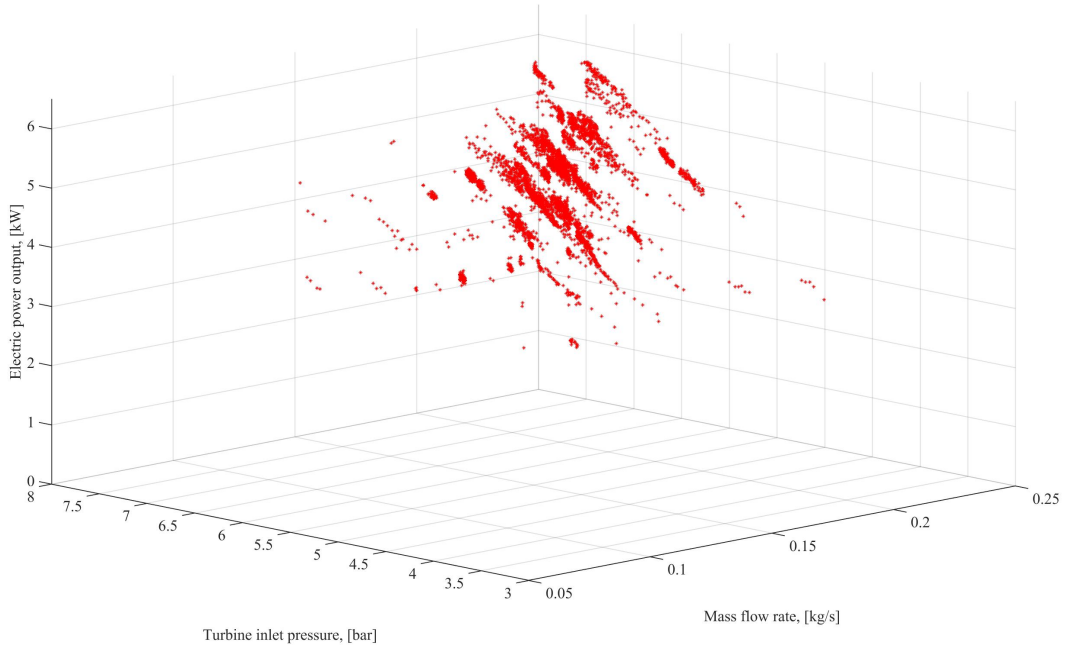

Figure 6: Electric power output as a function of turbine inlet pressure and working fluid mass flow rate.

In the experiments, one of the most important issues was to evaluate losses in the process components, especially in the turbogenerator. Power and loss distributions in turbogenerator were evaluated both experimentally and through computations. An example of power and loss distribution is presented in Figure 7 which shows the measured and calculated data as well as estimated data as a function of elapsed time during a test run. One of the most interesting issues is to compare the calculated electric power (grey curve) to the measured electric power (blue curve). The calculated electric power is based on the calculated turbine power (red curve) by taking into account the calculated mechanical losses (black curve) as well as the calculated feed pump power (yellow curve) and the estimated electrical losses (green curve). The turbine mechanical power was defined from the measured mass flow rate as well as by measuring the temperatures and pressures for the determination of the thermodynamic state values at the turbine inlet and outlet. The differences between the calculated electric power and the measured electric power was observed to be relatively high (from 1 to 2 kW on average). In general, the difference between the measured electric power output and the calculated electric power output was observed to be more pronounced as the TG rotational speed is approaching the design speed when compared to the conditions having lower TG rotational speeds. The

above-mentioned differences can mainly be explained by the mechanical losses or electrical losses in the turbogenerator being significantly higher than the calculated ones determined in the system design phase. One explanation for the high losses can be related to a high rotational speed in combination with possible presence of liquid working fluid surrounding the rotating parts. In addition, the uncertainties in flow rate as well as in turbine pressure and temperature measurements can lead to inaccuracy in the defined turbine mechanical power output in the analysis.

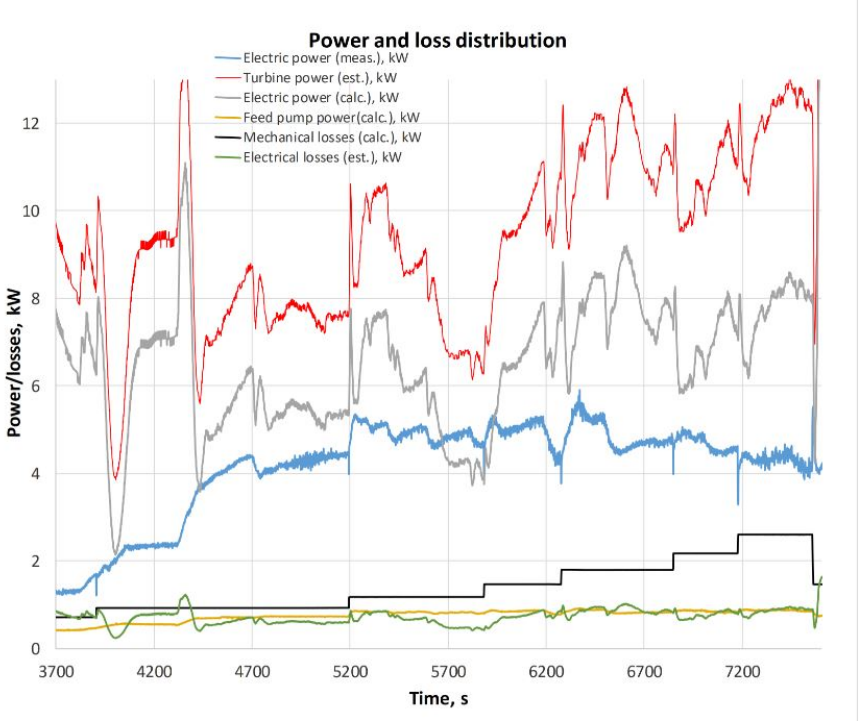

Figure 7: Example of power and loss distribution during a test run. Turbine inlet and outlet temperature as well as pressure measurements were used for defining enthalpy change over the turbine.

In general, as the turbogenerator speed was increased the mass flow rate through the turbine and the turbine inlet pressure were increased which also increased the turbine mechanical power output. On the other hand, the increase in the turbogenerator rotational speed also increased the mechanical losses and feed pump power consumption and as a result, the electric power output is not necessarily increased when approaching the system design speed. In general, the highest electric power outputs were measured with rotational speeds of about 75 % to 90 % of the design rotational speed. The moments where the turbogenerator rotational speed has been changed can be seen as changes in the values of calculated mechanical losses (black curve) in Figure 7.

In Figure 8a and 8b, the enthalpy and temperature drops over the turbine as a function of turbine pressure ratio are presented. The results are shown as data points based on the computational analysis of

the measured data obtained from several test runs with the TG rotational speed ranging from about 20 000 rpm to 31 300 rpm. There is a slight or moderate increasing trend in the isentropic enthalpy drop as well as in the isentropic temperature drop over the turbine as the turbine pressure ratio increases (small red markers) but significantly greater deviations are related to the data points of the enthalpy and temperature drop based on the measurements (small blue markers). In Figure 8a and 8b, the blue markers of upward-pointing triangle type refer to the turbine design values. Based on averaging the data related to the data points shown in Figure 8a, the turbine isentropic efficiency close to 70 % was determined and in the majority of the measured points the turbine efficiency was ranging from 60 % to 85 %. The turbine isentropic efficiency defined from the measurements as a function of turbine pressure ratio is shown in Figure 9 for operating conditions with TG rotational speeds ranging from 26 500 rpm to 31 300 rpm and being relatively close to the TG rotational speed at the system design operating condition. For the measurement points with high TG rotational speeds an average turbine isentropic efficiency of about 75 % was estimated.

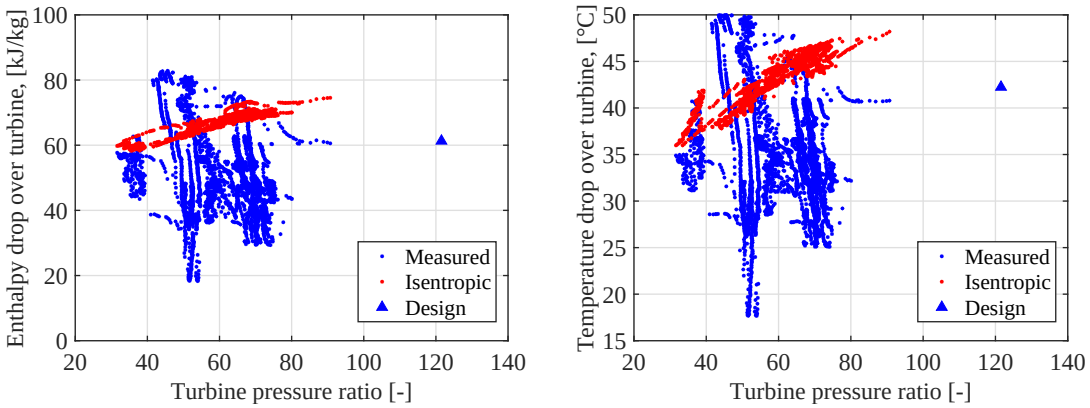

Figure 8: (a) Calculated enthalpy drop over the turbine based on the measured turbine inlet and outlet conditions and isentropic enthalpy drop and (b) measured temperature drop and isentropic temperature drop for the respective measurement points.

It was observed that defining the turbine efficiency from the experimental data is sensitive especially on the measured turbine outlet temperature as despite high pressure ratio over the turbine the temperature drop remains moderate. Even a small change of 1 K to 2 K in the measured turbine outlet temperature results in significant change in the defined turbine isentropic efficiency and highlights the importance of measuring the turbine outlet temperature with high accurately. The turbine efficiency is not as sensitive on small changes in turbine inlet temperature or inlet or outlet pressure. In general, the measured turbine outlet temperature had some fluctuations in the experiments, especially in conditions with TG rotational speeds ranging from 20 000 rpm to 25 000 rpm. It was observed from the experimental data that some of the data points of the enthalpy and temperature drop are even located above the trend tracks of the

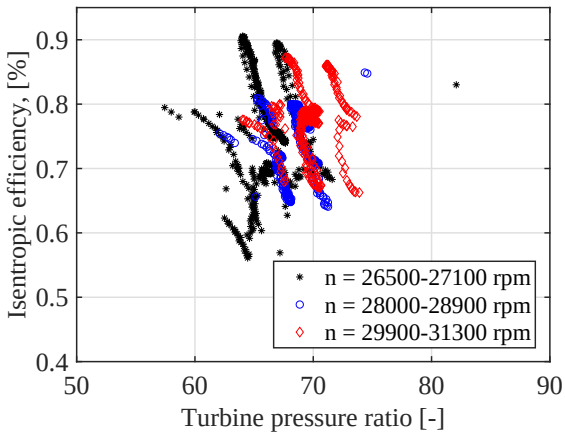

Figure 9: Turbine efficiency with TG rotational speeds ranging from 26 500 to 31 300 rpm.

isentropic enthalpy and isentropic temperature drop. Those points as well as the points close to the above-mentioned isentropic trend tracks were treated as outliers and they were left out from the determination of the turbine isentropic efficiency. The high measured temperature drop over the turbine in some of the operating conditions could have been caused by the liquid working fluid leaking from the turbogenerator to the turbine outlet and cooling down the flow temperature at the turbine outlet or otherwise disturbing the turbine outlet temperature measurement.

In the test runs, the turbine pressure ratio was ranging from 40 to 75 at the majority of the measured conditions and thus, the turbine design pressure ratio of over 100 was not reached. The turbine outlet pressure was measured to be higher than the outlet pressure used in the turbine design. This was estimated to be caused mainly by the higher measured pressure drop between the turbine outlet and the condenser than was evaluated in the system design phase as well as by the higher measured condenser pressure when compared to the results of the thermodynamic models of MDM at the respective measured condenser temperatures. As MDM has a very low condensing pressure at the studied condensing conditions, even a small rise in the condenser pressure or in the turbine outlet pressure can significantly reduce the turbine pressure ratio. One possibility for the high measured condensing pressure could be a presence of small amounts of non-condensable gases or other impurities, e.g. water or other light-molecule substances in the system that have a higher condensing pressure when compared to MDM.

In order to increase the reliability of the measurements and to have better understanding on the loss distribution of the turbogenerator the following tasks and improvements are worth considering in the future.

• Study of the liquid working fluid leakage flows from the main feed pump and from the bearings of the turbogenerator.

• Ensure sufficient draining of liquid working fluid from the turbogenerator to avoid unnecessary accumulation of liquid in the spaces surrounding the rotating parts.

• Additional temperature and pressure measurements especially at the turbine outlet as well as between the turbine stator and rotor for a more detailed analysis of turbine performance.
• Additional flow rate measurement of vapor working fluid at the turbine inlet to improve the reliability of the flow rate measurements.
• Evaluation of the effect of possible impurities or non-condensable gases in the working fluid on the thermodynamic performance of the system.

4. Conclusions

A small-scale ORC system having a high operating temperature was investigated and the technical potential of using high rotational speed and supersonic turbomachinery in small-scale and high expansion ratio ORC applications was confirmed experimentally. Siloxane MDM was used as the working fluid in the experiments. Based on the results, the main components of the turbogenerator, namely the main feed pump, generator and the supersonic radial turbine were capable to operate at the targeted turbogenerator rotational speed range of 12 000 rpm to 31 000 rpm. According to flow rate, pressure and temperature measurements, the turbine was analyzed to be able to produce mechanical power outputs that are close to the system design value of about 12 kW, although the turbine design pressure ratio was not fully reached in the experiments. This was mainly due to the higher measured pressure drop between the turbine outlet and the condenser as well as the higher condenser pressure when compared to the design values. In the analysis of turbine performance, it was observed that the majority of the measured temperature drops and enthalpy drops were in the expected range and generally in line with the results of numerical models for MDM at the studied operating conditions. Despite the high pressure ratio over the turbine, the temperature and enthalpy drops are moderate due to high molecular weight of the fluid. This feature also highlights the need for using a recuperator in the system. It was also observed that the internal power consumption and the turbogenerator losses have a significant influence on the system electric power output. The maximum electric power output that was reached in the experiments was approximately 6 kW that is about 1.5 kW to 2 kW lower than the power output that was estimated during the construction and design of the experimental system. This was estimated to be caused by greater losses or higher internal power consumption of the turbogenerator when compared to the computationally defined ones in the ORC system design phase. The turbogenerator losses were observed to be significantly high especially when the turbogenerator rotational speed is approaching the design rotational speed. This highlights the need for further investigations and detailed loss distribution analysis for small-scale ORC turbogenerators having high rotational speeds in order to improve the performance and feasibility of such ORC systems in the future.

Acknowledgements

Funding for the research work was received partly from LUT University, partly from Business Finland under project "Integrated Energy Solutions to Smart and Green Shipping", and partly from Academy of Finland under project "Loss mechanisms in expanding supercritical fluids" (grant number 323248).

References

[1] Quoilin, S., Van Den Broek, M., Declaye, S., Dewallef, P., and Lemort, V. (2013) Techno-economic survey of Organic Rankine Cycle (ORC) systems. *Renewable and Sustainable Energy Reviews*, 22, 168-186.

[2] Colonna, P., Casati, E., Trapp, C., Mathijssen, T., Larjola, J., Turunen-Saaresti, T., and Uusitalo, A. (2015). Organic Rankine cycle power systems: from the concept to current technology, applications, and an outlook to the future. *Journal of Engineering for Gas Turbines and Power*, 137(10), 100801.

[3] Sprouse III C. and Depcik C. (2013) Review of organic Rankine cycles for internal combustion engine exhaust waste heat recovery. *Applied Thermal Engineering*, 51(1-2),711-722.

[4] Invernizzi C., Iora P., and Silva P. (2007) Bottoming micro-Rankine cycles for micro-gas turbines. *Applied Thermal Engineering*, 27(1),100-110.

[5] Qiu G., Shao Y., Li J., Liu H., and Riffat S.B. (2012) Experimental investigation of a biomass-fired ORC-based micro-CHP for domestic applications. *Fuel*, 96,374-382.

[6] Bracco R., Clemente S., Micheli D., and Reini M. (2013) Experimental tests and modelization of a domestic-scale ORC (Organic Rankine Cycle). *Energy*, 58,107-106.

[7] Quoilin, S., Declaye, S., Tchanche, B. F., and Lemort, V. (2011). Thermo-economic optimization of waste heat recovery Organic Rankine Cycles. *Applied Thermal Engineering*, 31(14),2885-2893.

[8] Maraver D., Royo J., Lemort V., and Quoilin S. (2014) Systematic optimization of subcritical and transcritical organic Rankine cycles (ORCs) constrained by technical parameters in multiple applications. *Applied energy*, 117, 11-29.

[9] Uusitalo, A., Turunen-Saaresti, T., Honkatukia, J., Colonna, P., Larjola, J. (2013). Siloxanes as working fluids for mini-ORC systems based on high-speed turbogenerator technology. *Journal of Engineering for Gas Turbines and Power*. Vol. 135.

[10] Weiss, A. P., Popp, T., Müller, J., Hauer, J., Brüggemann, D., and Preissinger, M. (2018). Experimental characterization and comparison of an axial and a cantilever micro-turbine for small-scale Organic Rankine Cycle. *Applied Thermal Engineering*, 140, 235-244.

[11] Uusitalo, A., Honkatukia, J., Turunen-Saaresti, T., and Grönman, A. (2018). Thermodynamic evaluation on the effect of working fluid type and fluids critical properties on design and performance of Organic Rankine Cycles. *Journal of Cleaner Production*, 188, 253-263.

[12] Weiss, A.P. (2015). Volumetric expander versus turbine- which is the better choice for small ORC plants. In 3rd International Seminar on ORC Power Systems, Oktober (pp. 12-14).

[13] Lemort, V., Guillaume, L., Legros, A., Declaye, S., and Quoilin, S. (2013) A comparison of piston, screw and scroll expanders for small scale Rankine cycle systems. In Proceedings of the 3rd International Conference on Microgeneration and Related Technologies, Naples, Italy, April 5-17.

[14] Song, P., Wei, M., Shi, L., Danish, S. N., and Ma, C. (2015) A review of scroll expanders for organic Rankine cycle systems. *Applied Thermal Engineering*,75,54-64.

[15] van Buijtenen J.P., Larjola J., Turunen-Saaresti T., Honkatukia J., Esa H. and Backman J. Design and validation of a new high expansion ratio radial turbine for ORC application. 5th European conference on Turbomachinery. Prague, 2003,March 17-22.

[16] Meroni, A., Robertson, M., Martinez-Botas, R., and Haglind, F. (2018). A methodology for the preliminary design and performance prediction of high-pressure ratio radial-inflow turbines. *Energy*, 164, 1062-1078.

[17] Uusitalo, A., Turunen-Saaresti, T., Guardone, A., and Grönman, A. (2014). Design and flow analysis of a supersonic small scale ORC turbine stator with high molecular complexity working fluid. In ASME Turbo Expo 2014: Turbine Technical Conference and Exposition (pp. V03BT26A004-V03BT26A004). American Society of Mechanical Engineers.

[18] Kang, S. H. (2012). Design and experimental study of ORC (organic Rankine cycle) and radial turbine using R245fa working fluid. *Energy*, 41(1), 514-524.

[19] Klonowicz, P., Borsukiewicz-Gozdur, A., Hanausek, P., Kryllowicz, W., and Brüggemann, D. (2014). Design and performance measurements of an organic vapour turbine. *Applied Thermal Engineering*, 63(1), 297-303.

[20] Seume, J. R., Peters, M., and Kunte, H. (2017). Design and test of a 10kW ORC supersonic turbine generator. Journal of Physics: Conference Series (Vol. 821, No. 1, p. 012023). IOP Publishing.

[21] Head, A. J., De Servi, C., Casati, E., Pini, M., and Colonna, P. (2016). Preliminary design of the ORCHID: a facility for studying non-ideal compressible fluid dynamics and testing ORC expanders. In ASME Turbo Expo 2016: Turbomachinery Technical Conference and Exposition. American Society of Mechanical Engineers Digital Collection.

[22] Uusitalo A., Honkatukia J., and Turunen-Saaresti T. (2017) Evaluation of a small-scale waste heat recovery organic Rankine cycle. *Applied energy*, 192 (2017): 146-158.

[23] Uusitalo, A. (2014). Working fluid selection and design of small-scale waste heat recovery systems based on organic Rankine cycles. Lappeenranta University of Technology, Doctoral Thesis.

[24] Lemmon, E. W., Huber, M. L., and McLinden, M. O. (2010). NIST Standard Reference Database 23, NIST Reference Fluid Thermodynamic and Transport Properties, REFPROP, version 9.0. Standard Reference Data Program.